Electronic Supplementary Material (ESI) for Journal of Materials Chemistry A.
This journal is © The Royal Society of Chemistry 2017

Supporting Information

Comparison of alkene hydrogenation in carbon nanoreactors of different diameters: probing the effects of nanoscale confinement on ruthenium nanoparticle catalysis

Mehtap Aygün, Craig T. Stoppiello, Maria A. Lebedeva, Emily F. Smith, Maria del Carmen Gimenez-Lopez, Andrei N. Khlobystov and Thomas W. Chamberlain.

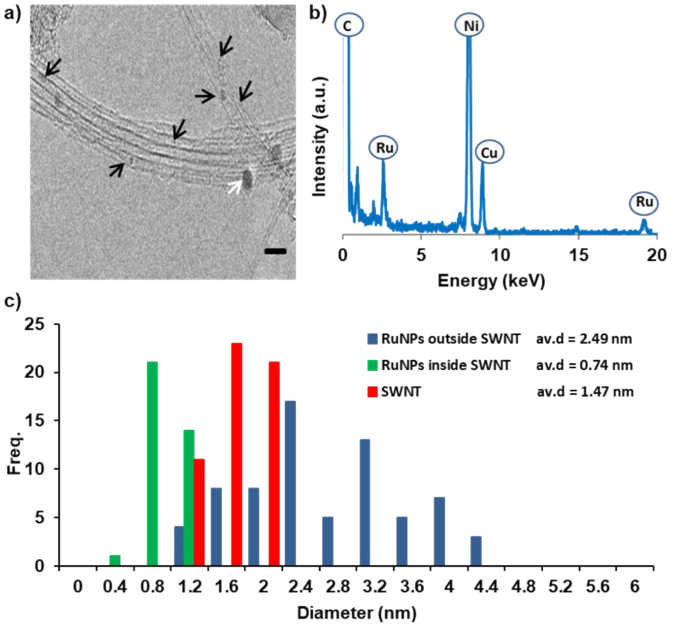

Figure S-1. **a)** HRTEM image of RuNPs@SWNT loaded with 3.1% of Ru by wt. Black and white arrows indicate RuNPs inside and outside of the SWNT respectively. **b)** EDX spectrum showing the composition of RuNP@SWNT. Ni peaks are from the synthetic process of SWNT manufacture and the Cu from the TEM grid, respectively. **c)** A histogram showing the size distribution of SWNT (red), RuNPs located inside the SWNT (green) and RuNPs located outside the SWNT (blue). Scale bar: 2 nm.

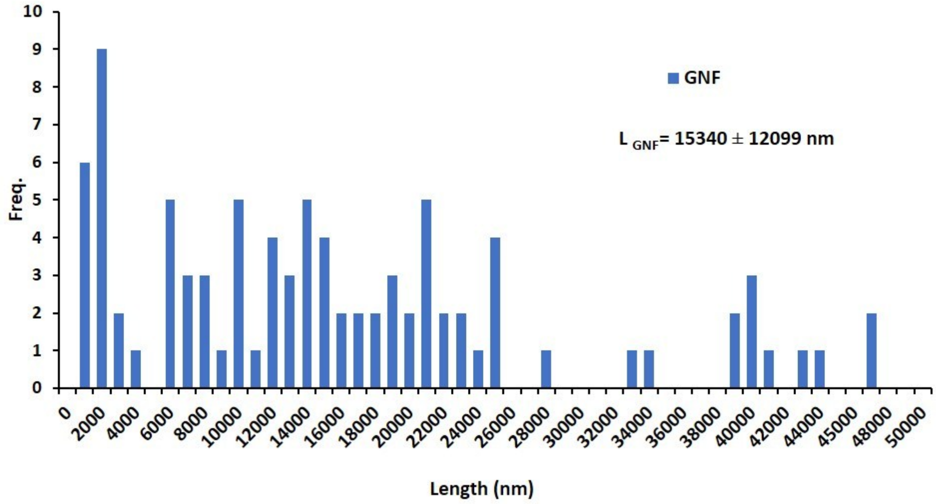

Figure S-2. A histogram showing the size distribution of GNF used to fabricate RuNPs@GNF, L_{GNF} = 15340 ± 12099 nm.

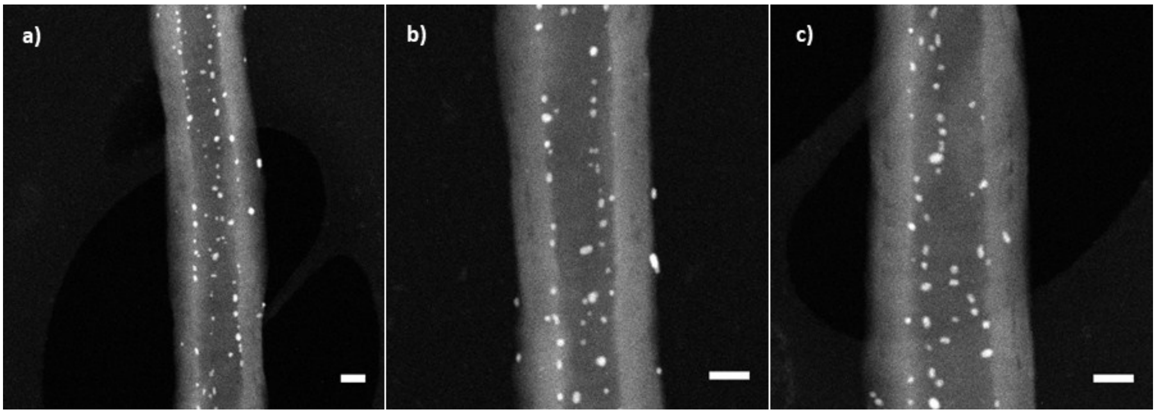

Figure S-3. a-c) Dark-field scanning TEM images of RuNPs@GNF loaded with RuNPs. Only a very small amount of Ru material (~7 % approximated by TEM analysis), is located on the outer surface of the GNF so all conversion is assumed to be a result of reactions catalysed by RuNPs on the inside of the GNF. Scale bar: 20 nm in all cases.

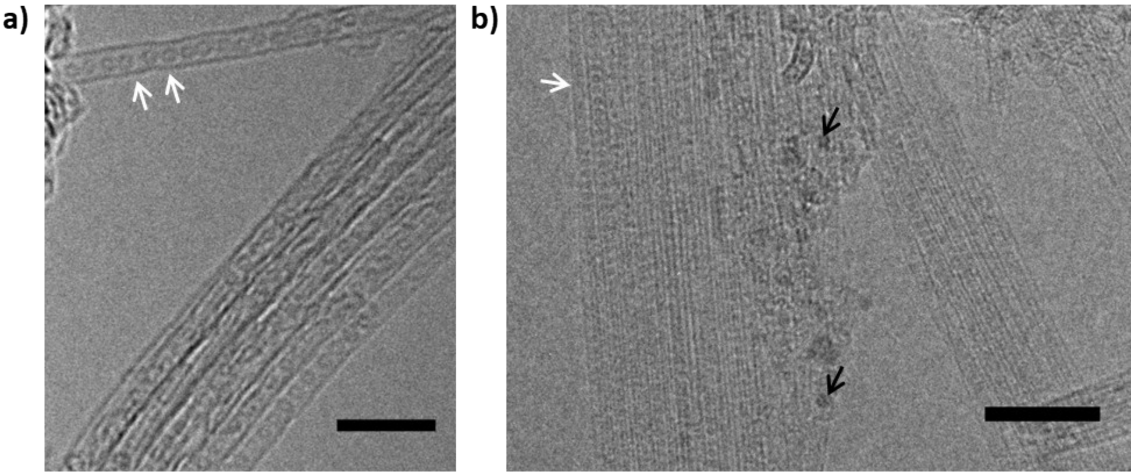

Figure S-4. a) HRTEM image of C_{60}@SWNT support material. White arrows show individual C_{60} molecules, observed as circles ~0.7 nm in diameter, filling the available space within the internal channel of the SWNT. The filling rate is observed to be ~100%, *i.e.* all SWNT are seen to be completely full of C_{60} molecules. Scale bar: 5 nm. **b)** HRTEM image of RuNPs/C_{60}@SWNT. White arrow shows a SWNT completely filled with C_{60} molecules, whilst black arrows highlight the individual RuNPs located on the outer surface of the C_{60}@SWNT support. Scale bar: 10 nm

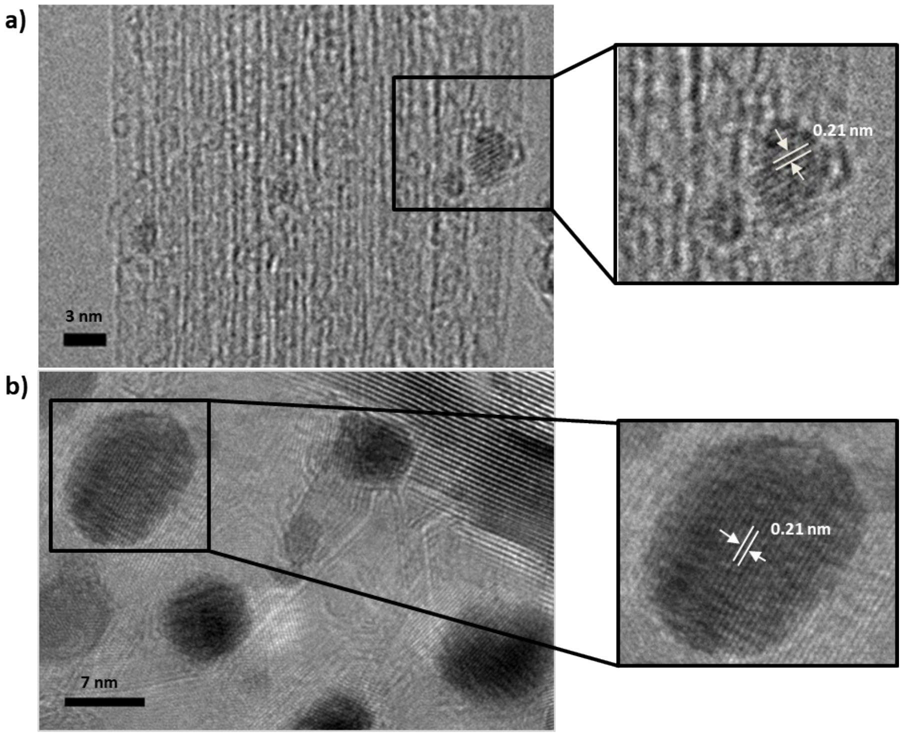

Figure S-5. HRTEM images of **a)**, RuNPs@SWNT, and **b)**, RuNPs@GNF with enlarged regions showing the Ru [002] lattice spacing (d = 0.21 nm) of individual, hcp structured, metallic NPs which correspond to the 2θ peak centred at 42.2° in the XRD for both materials.

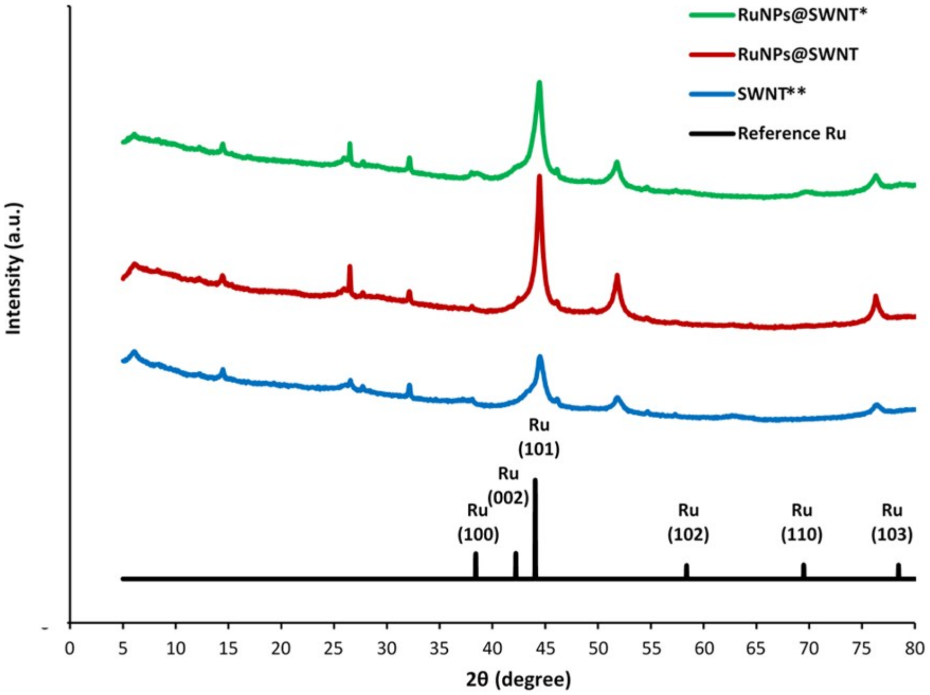

Figure S-6. Powder XRD patterns of RuNPs@SWNT (1.6 % Ru by wt.) and RuNPs@SWNT* (10 % Ru by wt.) and SWNT (**SWNT was annealed at 380 °C for 20 min prior to use) together with reference patterns for Ru.[S-1]

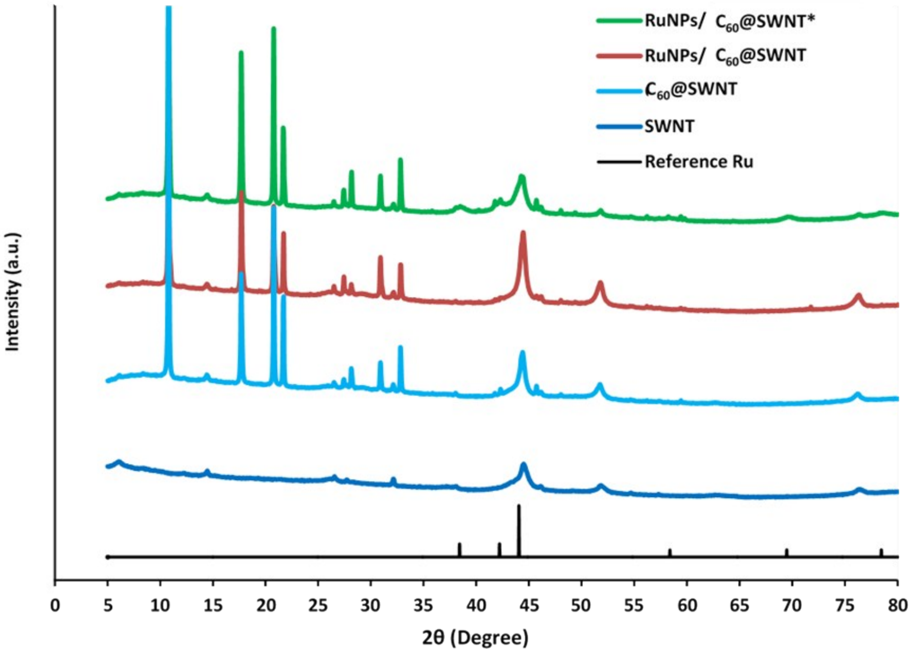

Figure S-7. Powder XRD patterns of SWNT, C_{60}@SWNT, RuNPs/C_{60}@SWNT (3.1 % Ru by wt.) and RuNPs/C_{60}@SWNT * (10 % Ru by wt.) together with reference patterns for Ru.[S-1]

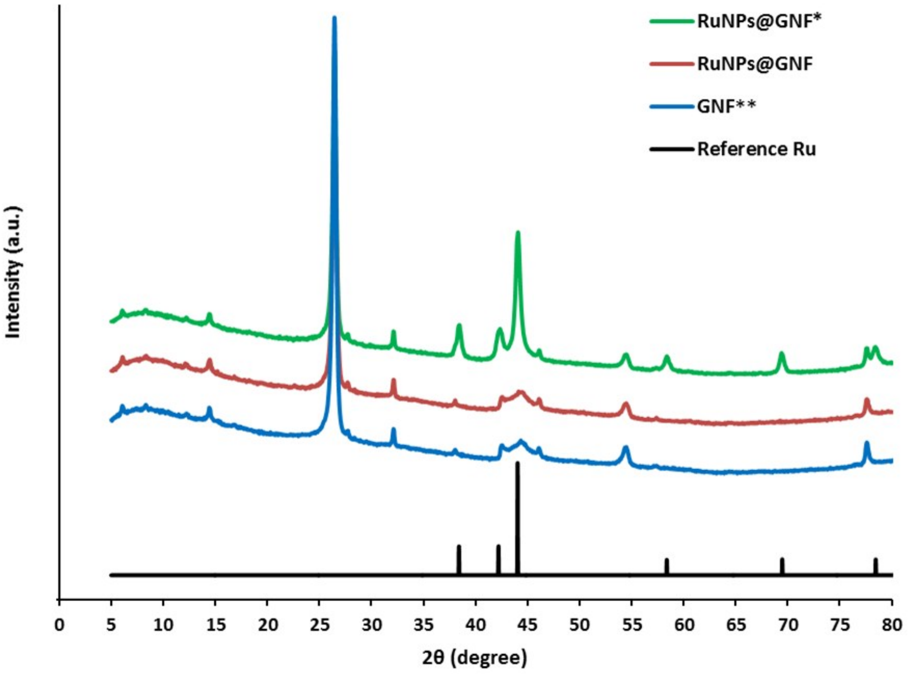

Figure S-8. Powder XRD patterns of RuNPs@GNF (1 % Ru by wt.) and RuNPs@GNF* (10 % Ru by wt.) and GNF (**GNF was was annealed at 450 °C for 1 h prior to use) together with reference patterns for Ru.[S-1]

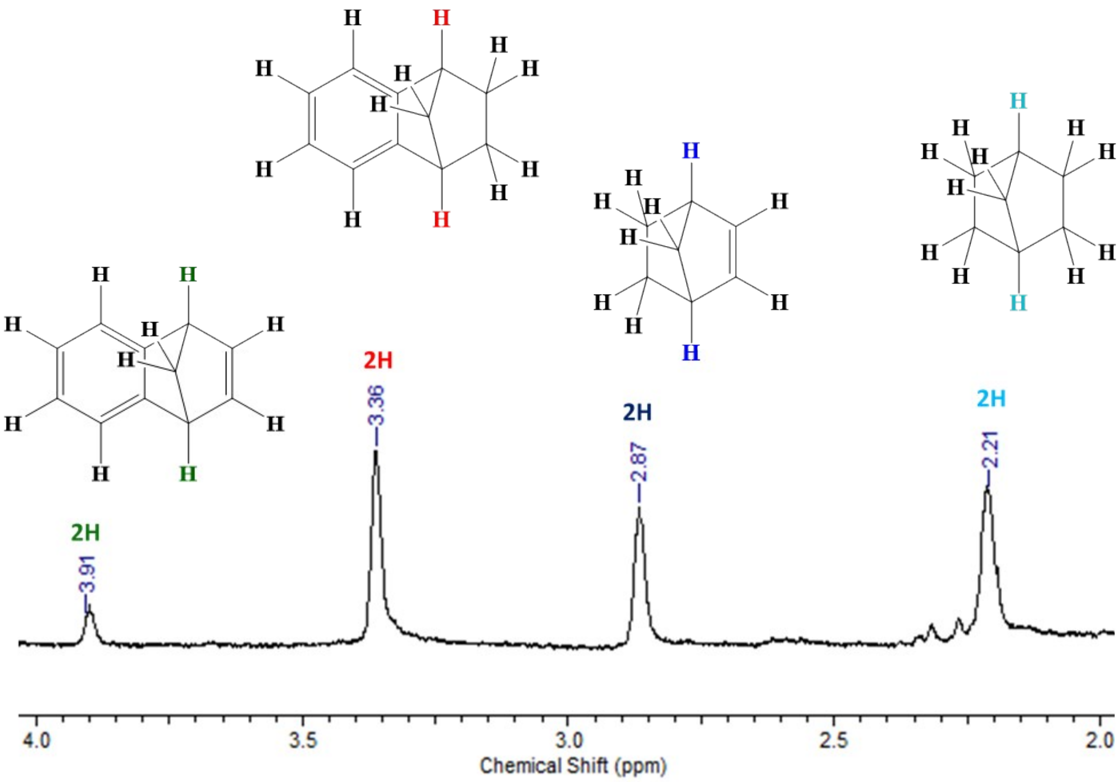

Figure S-9. ^{1}H NMR of spectrum of the reaction mixture of catalytic hydrogenation of norbornene vs. benzonorbornadiene, where bridge hydrogens of the starting material of norbornene gives a multiplet at 2.87 pmm (green) was compared in the product of norbornane giving three multiplets at 2.21 ppm (red) and bridge hydrogens of the starting material of benzonorbornadiene gives a multiplet at 3.91 pmm (dark blue) was compared in the product of 1,4-Methano-1,2,3,4-tetrahydronaphthalene giving a multiplet at 3.36 (blue).

X-ray photoelectron spectroscopy

XPS experimental details

Samples were analysed using the Kratos AXIS ULTRA with a mono-chromated Al kα X-ray source (1486.6 eV) operated at 10 mA emission current and 12 kV anode potential (120 W.) A charge neutralizer filament was used to prevent surface charging. Hybrid –slot mode was used measuring a sample area of approximately 0.5 mm^2. The analysis chamber pressure was better than 5 x 10^{-9} mbar. Three areas per sample were analysed. A wide scan at low resolution (1400 - -5 eV binding energy range, pass energy 80 eV, step 0.5 eV, sweep time 20 minutes) These were used to estimate the total atomic % of the detected elements. High resolution spectra at pass energy 20 eV with step of 0.1 eV, sweep times of 10 minutes each were also acquired for photoelectron peaks from the detected elements and these were used to model the chemical composition. The high resolution spectra were charge corrected to the C 1s peak set to 285 eV.

Casaxps (version 2.3.18dev1.0x) software was used for quantification and spectral modelling.

Detector mode: The ULTRA was used in FAT (fixed analyser transmission) mode, with pass energy of 80 eV for wide scans and pass energy 20 eV for high resolution scans. A Hybrid magnetic/electrostatic lens mode is used for maximum electron signal. The magnetic immersion lens system allows the area of analysis for to be defined by apertures, a 'slot' aperture of 300 x 700 µm for wide/survey scans and high resolution scans. The take-off angle for the photoelectron analyser is 90˚ and acceptance angle of 9˚ for hybrid lens mode utilised.

Calibrations: The energy range of the XPS was calibrated using Cu, Ag and Au samples. The resolution for the photoelectron detector was based on Ag $3d_{5/2}$ peak FWHM of less than 0.55 eV at PE 20 in hybrid slot mode. The transmission function of the instrument was calibrated using a clean gold sample for all lens modes and pass energies. Last date of calibrations: Energy range, resolution check and Transmission function, July 2013, Kratos Factory settings.

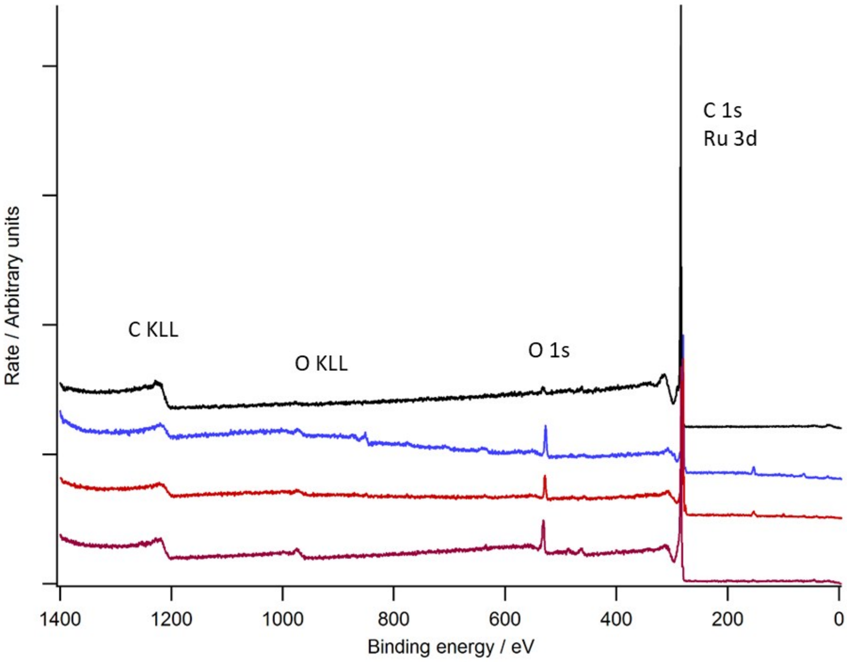

Figure S-10. XPS data for RuNPs@GNF (black), RuNPs@SWNT (blue), RuNPs/C_{60}@SWNT (red) and Ru/C (purple) collected with a monochromated Al Kα X-ray source (1486.6 eV) operated at 10 mA emission current and 12 kV anode potential (120 W). Oxygen peak is associated with defects in the carbon supports.

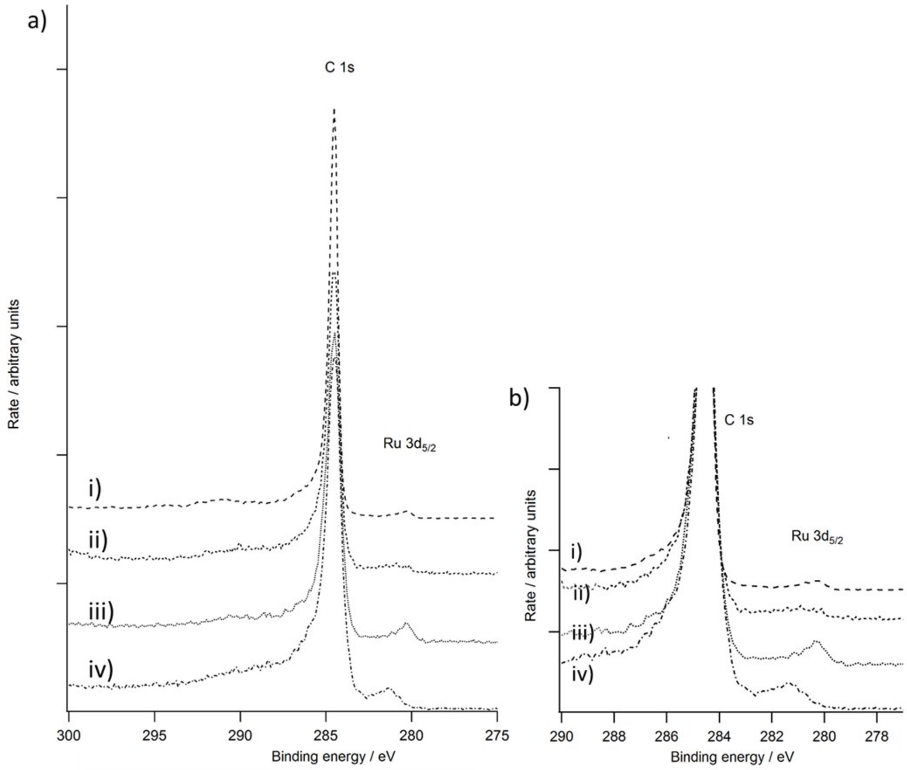

Figure S-11. a-b) Enlarged regions of the XPS data for i) RuNPs@GNF, ii), RuNPs@SWNT, iii) RuNPs/C_{60}@SWNT, and iv) Ru/C control showing the characteristic Ru 3d 5/2 peak at 280.2 eV for the all carbon nanostructure supported catalysts which is consistent with the binding energy for metallic Ru reported previously.[S-2]

TGA and ICP-OES to determine Ru loading for RuNPs@SWNT and GNF

TGA was used to measure the content of Ru metal within the RuNPs@GNF catalyst. As pure GNFs do not contain additional residual metal species it is possible to equate the residual weight after oxidation of the carbon in RuNPs@GNF samples to the loading of Ru metal (see Figure S-12).

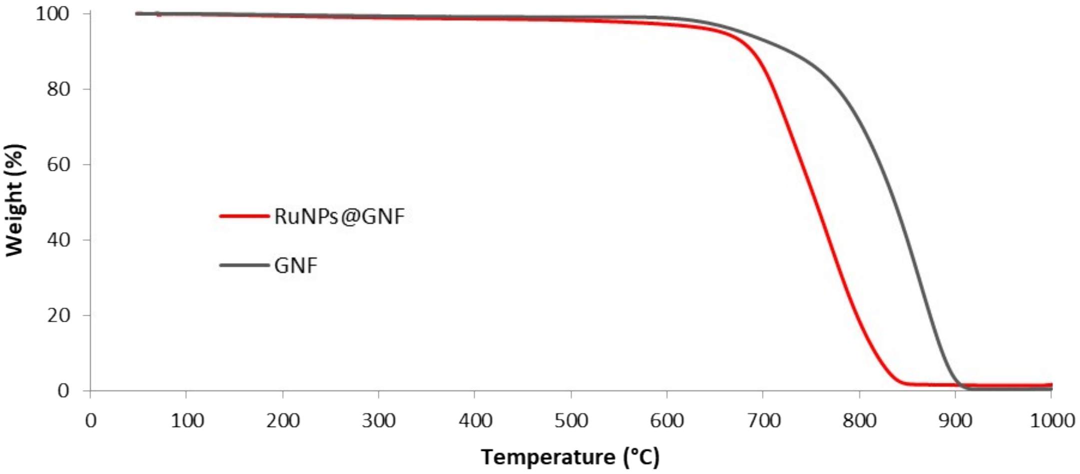

Figure S-12. TGA curves of GNF (blue) with 0.62% residual weight, and RuNPs@GNF (dark blue) with 1.6 % residual weight, which corresponds to 1 % wt. ± 0.1 of Ru in the carbon supported RuNP catalyst**.** Both measurements were carried out between 25-1000 °C in air at a heating rate of 10 °C/min.

In contrast, as the method of SWNT production results in the unavoidable presence of significant and inhomogeneous amounts of large, inert Ni/Y nanoparticles in the pure support (~40 %) this makes quantification of the amount of Ru present solely by TGA difficult. In addition, SWNT do not completely digest in strong acids making inductively coupled plasma optical emission spectroscopy (ICP-OES) of NT samples problematic. To address this the RuNPs@SWNT material was initially oxidised by TGA to remove the carbon material and the remaining residual metal was then digested in acid and analysed by ICP-OES using the following general method: RuNPs@SWNT (3 x 2 mg) were heated to 1000 °C in air in a TA Instruments TGA-SDTQ600 analyser to oxidise and remove all of the carbon material and leave just the ruthenium metal in the alumina crucible (see Figure S-13). The residual material was then dissolved in HNO_3 (2 mL, 69 % HNO_3) with heating and stirring at 50 °C for 6 hours and the resultant solution was diluted with ultrapure water to make a dilute HNO_3 solution (10% by volume in water). ICP-OES was used to determine the Ru content of the solution using a Perkin Elmer, Optima 2000 DV ICP-OES with S10 autosampler with an axial detection method at wavelengths of 240.272 and 349.894 nm. Calibration Ru solutions (0.005, 0.01, 0.05 and 0.1 mg mL^{-1}) were prepared using a Ru standard (VWR Chemicals) and 10% HNO_3, and gave a linear plot with an R coefficient of 0.999999. Blanks showed 0.00 mg L^{-1} of Ru. Corrected concentrations were measured as 0.9, 1.2 and 1.2 mg of Ru per litre for each sample, which correlates to Ru loadings of 1.33, 1.58 and 1.76 % Ru respectively for the three RuNPs@SWNT sample (average = 1.55 % Ru by wt.), see Table S-1.

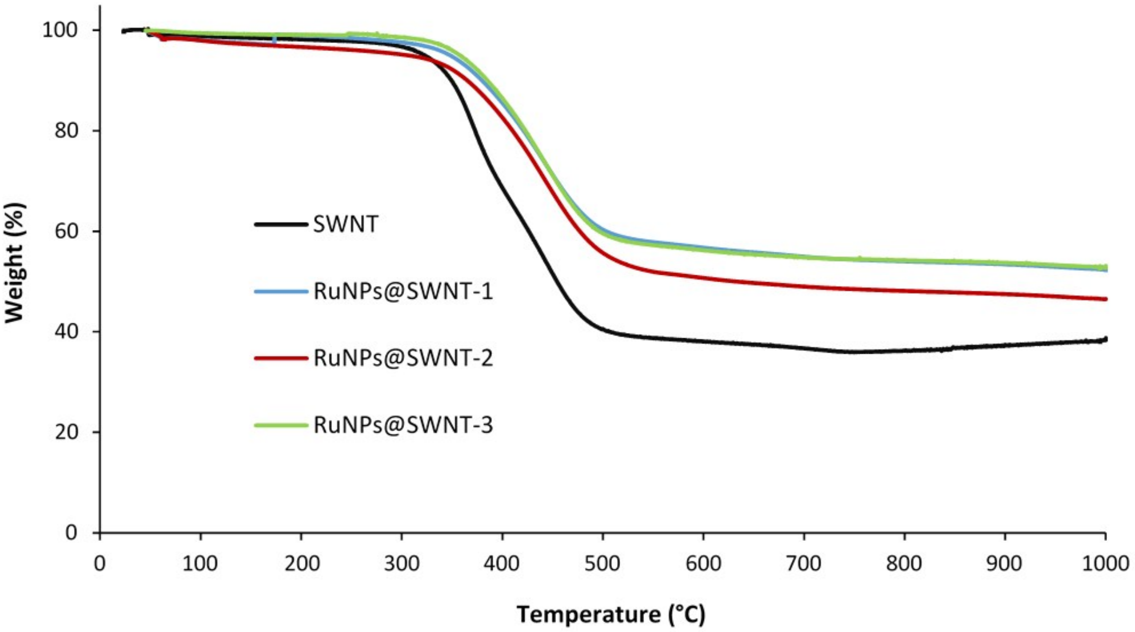

Figure S-13. TGA curves of SWNT and three 5 mg samples of RuNPs@SWNT (labelled 1, 2 and 3). All measurements were carried out between 25-1000 °C in air at a heating rate of 10 °C/min.

Table S-1. Data showing the precise loading of Ru metal in RuNPs@SWNT catalyst calculated by TGA and ICP-OES.

	Amount of material before TGA / mg	**Amount of Ru by ICP-OES / mg.L^{-1}**	**Amount of Ru by TGA and ICP-OES / wt. %**	**Average amount of Ru by TGA and ICP-OES / wt. %**
RuNPs@SWNT-1	1.345	0.9	1.36	**1.55**
RuNPs@SWNT-2	1.502	1.2	1.58	
RuNPs@SWNT-3	1.36	1.2	1.76	

TON Calculations

Turnover numbers (TONs) in molecules per active site were calculated using the previously reported method[S-3] as follows;

Table S-2. Experimentally determined and theoretically calculated values used to approximate the TON of product molecules per active site for all carbon supported ruthenium catalysts.

Catalyst	**RuNPs@SWNT**	**RuNPs/C$_{60}$@SWNT**	**RuNPs@GNF**	**Ru/C**
Average RuNP size[a] / nm	0.74 ± 0.18	2.56 ± 0.62	3.58 ± 1.14	6.63 ± 2.45
Surface area of 1 RuNP[b] / nm^2	1.72	20.60	40.28	138.15
Number of Ru NPs in the catalyst (equiv. to 0.0017 mmol% of Ru per reaction)[c]	3.28×10^{16}	1.59×10^{15}	1.87×10^{14}	9.13×10^{13}
Active Ru surface area of the catalyst / m^2 g^{-1}	7.46	4.31	1.00	2.69
Surface area of the Ru NPs used in the reaction / m^2	0.04	0.02	0.006	0.009
Number of Ru active sites in the catalyst used in the reaction[d]	1.85×10^{17}	1.07×10^{17}	2.46×10^{16}	4.13×10^{16}
Norbornene molecules produced[e]	5.48×10^{20}	7.22×10^{19}	2.77×10^{20}	3.07×10^{20}
TON / molecules of product per active site	2959	675	11216	7428

[a] Determined experimentally by HRTEM. [b] The active Ru surface area of the RuNPs catalysts was calculated assuming all of the NPs to be the average diameter measured by TEM, see Table 1. [c] By treating the nanoparticles as perfect spheres and knowing the mass of Ru metal in the sample enabled the number of NPs to be calculated. The surface area occupied by an individual Ru atom on the nanoparticle surface was approximated to be 0.89 nm^2 and assumes that the surface of the Ru nanoparticles is a 1:1 mix of 001 and 100 crystallographic planes.[S-4] [d] Calculated using the true active surface areas, details of how this was calculated are shown below. [e] Calculated from the single hydrogenation of norbornene in which RuNPs@carbon nanoreactor (0.17 mol% of Ru) and alkene substrate (1 mmol) with H_2 (10 bar) and CO_2 (100 bar) and heated to 110 °C for 24 hour and the resultant material was analyzed by ^{1}H NMR spectroscopy.

Calculations of theoretical surface areas and comparison with BET surface area values

RuNPs in all samples was assumed to be perfectly spherical in shape and have a diameter equal to the mean diameter measured experimentally by HRTEM.

For RuNPs@SWNT;

Atomic radius of a Ru atom= 0.134 nm

Surface area of a Ru atom = 4*(22/7)*(0.134^2)= 0.225732571 nm2 = 2.25732571*10^$^{-19}$ m^2

An average diameter of RuNP in SWNT= 0.74 nm (measured from HRTEM).

Volume of a RuNP = (4/3)*22/7*(0.74/2)^3= 0.21226 nm^3= 2.1226*10^{-22} cm^3.

Density of Ru = 12.45 g/cm^3.

Mass of a RuNP = 2.1226*10^{-22} *12.45 =~ 2.64*10^{-21} g.

Mass of RuNPs@SWNT =0.0056 g.

Mass of Ru in RuNPs@SWNT (1.55 % Ru by wt.) =0.0000868 g.

Number of all RuNPs = 0.0000868/2.64*10^{-21} = ~3.28*10^{16}.

Atomic surface area of a RuNP = 4*22/7*(0.74/2)^2 = 1.72 nm^2=1.72*10^{-18} m^2.

Total surface area of all RuNPs = 3.28*10^{16}*1.72*10^{-18}= 0.057 m^2.

Active surface area of all RuNPs (only 73.93% of surface atoms are active[S-5]) = 0.057*0.7393= 0.04179 m^2

Number of active Ru sites in RuNPs@SWNT used in the reaction

= Active surface area of all RuNPs / Surface area of a Ru atom = 0.04179/ 2.25732571*10^$^{-19}$= 1.8513*10^^{17}

Active surface area of Ru atoms per gr RuNPs@SWNT = 0.04179 m^2 / 0.0056 g = ~7.46 m^2/g

Theoretical surface area of SWNT (both internal and external surface) = 1315*2 =2630 m^2/g.[S-6]

Theoretical surface area of RuNPs@SWNT = 7.46 + 2630 = 2637.46 m^2/g.

The theoretical surface area of C$_{60}$@SWNT, RuNPs/C$_{60}$@SWNT, GNF, RuNPs@GNF and Ru/C were also calculated using the same calculations showed above (Table S-3, below).

Table S-3. Theoretical and BET surface area calculations for SWNT, RuNPs@SWNT, C_{60}@SWNT. RuNPS/C_{60}@SWNT, GNF, RuNPs@GNF and commercial Ru/C.

Material	Theoretical Surface Area / m^2/g	BET Surface Area / m^2/g
SWNT	2630	507.90
RuNPs@SWNT	2637.46	351.94
RuNPs in RuNPs@SWNT	7.46	N/A
C_{60}@SWNT	1315	120.99
RuNPs/C_{60}@SWNT	1319.31	164.82
RuNPs in RuNPs/C_{60}@SWNT	4.31	44.17
GNF	35	12.08
RuNPs@GNF	35.99	28.53
RuNPs in RuNPs@GNF	35.99	16.45
Carbon Black	N/A	900*
Ru/C	2.69	929.41
RuNPs in Ru/C	N/A	29.41

Pore size distribution curves

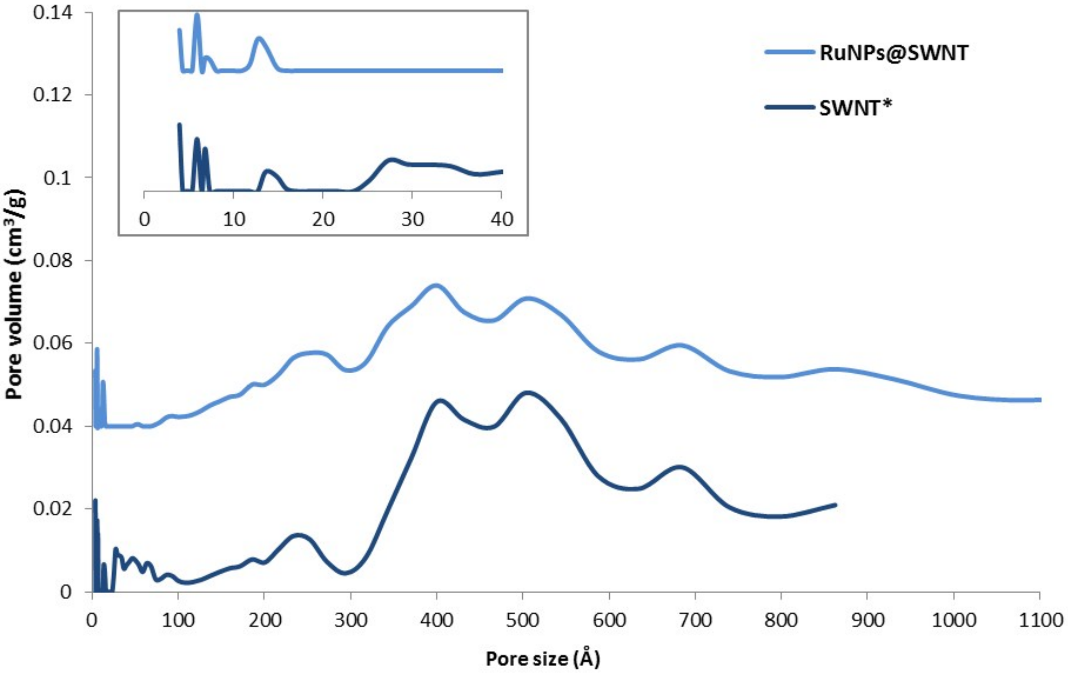

Figure S-14. Pore size distribution curves of SWNT (*SWNT was annealed at 380 °C for 20 min prior to use) and RuNPs@SWNT.

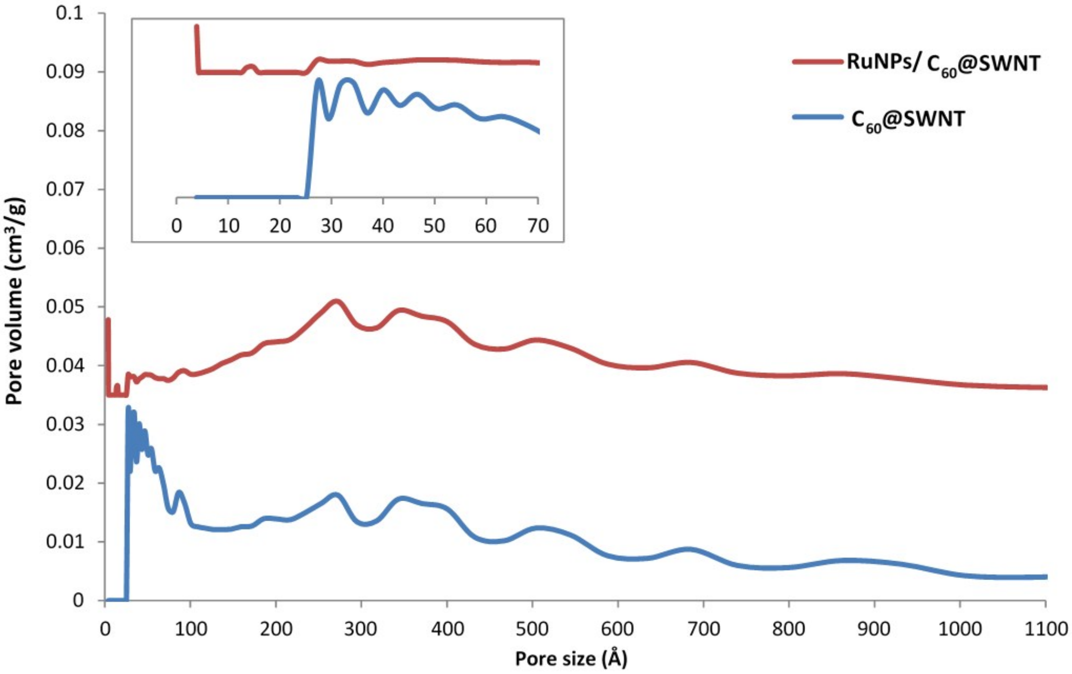

Figure S-15. Pore size distribution curves of C_{60}@SWNT and RuNPs/C_{60}@SWNT.

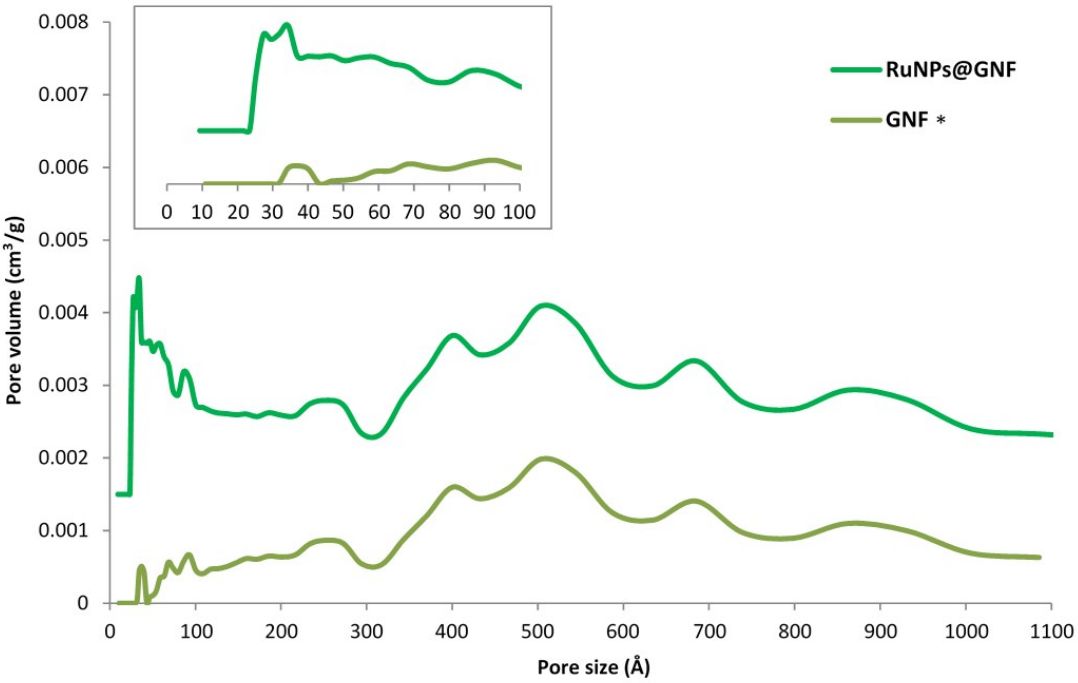

Figure S-16. Pore size distribution curves of GNF (*GNF was annealed at 450 °C for 1 h prior to use) and RuNPs@GNF.

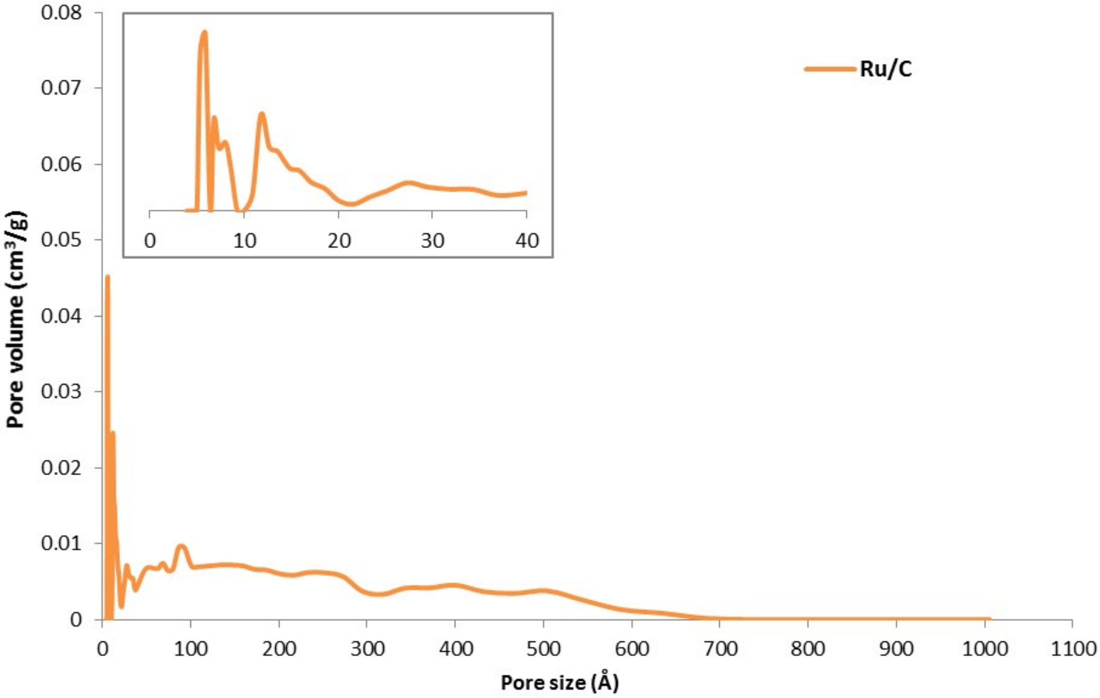

Figure S-17. Pore size distribution curves of commercial Ru/C.

Table S-4. Pore volume and size distribution SWNT, RuNPs@SWNT, C_{60}@SWNT, RuNPS/C_{60}@SWNT, GNF, RuNPs@GNF and commercial Ru/C.

Catalyst	**Pore volume, cm³/g**	**Pore size, Å**
RuNPs@SWNT	0.610758	5.89/6.79/12.68/252
SWNT	0.716652	11.79/252/400/503
RuNPs@GNF	0.062854	25.1/93.1/252/503
GNF	0.023237	34/86/252/503
RuNPs/C_{60}@SWNT	0.374275	14.83/27.34/93.10/272/343/504
C_{60}@SWNT	0.248492	27.34/34.31/40.03/46.64/93.10/272/343/504
Ru/C	0.7382	5.89/6.79/11.79/27.34

References

[S-1] H. E. Swanson, R. K. Fuyat and G. M. Ugrinic, *National Bureau of Standards (U.S.), Circular*, 1955, **5**, 539.

[S-2] J. F. Moulder, W. F. Stickle, P. E. Sobol and K. D. Bomben, *1992 Handbook of X-ray Photoelectron Spectroscopy* (Perkin-Elmer, Minnesota) pp. 44 and 114.).

[S-3] T. W. Chamberlain, J. H. Earley, D. P. Anderson, A. N. Khlobystov and R. A. Bourne, ***Chem. Commun.*** 2014, **50**, 5200-5202.

[S-4] R. A. D. Betta, *Journal of Catalysis*, 1974, **34**, 57-60.

[S-5] S. Agarwal and J. N. Ganguli, RSC Adv., 2014, 11893-11898.

[S-6] A. Peigney, C. Laurent, E. Flahaut R. Bacsa and A. Rousset, *Carbon, Elsevier*, 2001, **39**, 507-514.